

**University of California**

**Ernest O. Lawrence  
Radiation Laboratory**

**TWO-WEEK LOAN COPY**

*This is a Library Circulating Copy  
which may be borrowed for two weeks.  
For a personal retention copy, call  
Tech. Info. Division, Ext. 5545*

**Berkeley, California**

## **DISCLAIMER**

This document was prepared as an account of work sponsored by the United States Government. While this document is believed to contain correct information, neither the United States Government nor any agency thereof, nor the Regents of the University of California, nor any of their employees, makes any warranty, express or implied, or assumes any legal responsibility for the accuracy, completeness, or usefulness of any information, apparatus, product, or process disclosed, or represents that its use would not infringe privately owned rights. Reference herein to any specific commercial product, process, or service by its trade name, trademark, manufacturer, or otherwise, does not necessarily constitute or imply its endorsement, recommendation, or favoring by the United States Government or any agency thereof, or the Regents of the University of California. The views and opinions of authors expressed herein do not necessarily state or reflect those of the United States Government or any agency thereof or the Regents of the University of California.

To be published in Physical Review Letters

UCRL-10003  
Limited distribution

UNIVERSITY OF CALIFORNIA  
Lawrence Radiation Laboratory  
Berkeley, California  
Contract No. W-7405-eng-48

DETERMINATION OF THE  $\Sigma$  PARITY

Robert D. Tripp, Mason B. Watson, and Massimiliano Ferro-Luzzi

December 26, 1961

---

DETERMINATION OF THE  $\Sigma$  PARITY\*

Robert D. Tripp, Mason B. Watson, Massimiliano Ferro-Luzzi†

Lawrence Radiation Laboratory  
University of California  
Berkeley, California

December 26, 1961

In a previous Letter we reported a hydrogen-bubble-chamber experiment on the  $K^-p$  interaction in the vicinity of 400-Mev/c incident  $K^-$  momentum.<sup>1</sup> The existence of an excited hyperon of 1520-Mev mass and 16-Mev full-width was established; the state was found to have isotopic spin 0, spin 3/2, even parity with respect to  $K^-p$ , and a  $\bar{K}N:\Sigma\pi:\Lambda Z\pi$  branching ratio of 3:5:1. In this Letter we report the study of the angular distributions and polarizations of the different  $\Sigma\pi$  charge states, from which we conclude that the  $KP\Sigma$  parity is odd.

The determination of the  $KP\Sigma$  parity in the reaction



rests on establishing the parity of the transition operator  $M$  defined by  $\psi_f = M \chi_i$  where  $\psi_f(\theta, \phi)$  is the final-state wave function and  $\chi_i$  is the initial spin function. For a reaction in which a new pair of particles is created,  $M$  may be either scalar or pseudoscalar. The problem can be conveniently discussed in terms of a generalization of the Minami transformation.<sup>2</sup> Defining  $\underline{k}_i$  and  $\underline{k}_f$  as unit vectors in the incident  $K^-$  and outgoing  $\pi$  directions, respectively, and  $\underline{n} = \underline{k}_i \times \underline{k}_f / |\underline{k}_i \times \underline{k}_f|$  as the unit normal to the scattering plane, one can write four expressions for  $M$  -- two scalar and two pseudoscalar. These are listed in column 1 of Table I. Here  $A$  and  $B$  are functions of the center-of-mass (c.m.) scattering angle  $\theta$  between the  $K^-$  and the  $\pi$ . For final  $S_{1/2}$ ,  $P_{1/2}$ , and  $P_{3/2}$  waves (abbreviated  $S$ ,  $P_1$ ,  $P_3$ ), they are<sup>3</sup>

$$A = \frac{1}{2K} [S + (2P_3 + P_1) \cos \theta] ; B = \frac{i}{2K} [(P_3 - P_1) \sin \theta]. \quad (2)$$

Since the operators  $\underline{\sigma} \cdot \underline{k}_i$  and  $\underline{\sigma} \cdot \underline{k}_f$  change the parities of all initial- and final-state partial waves, respectively, the transformation from the first to the second row represents the usual Minami transformation, whereas rows 3 and 4 represent transformations of either the initial- or final-state partial waves of row 1. Thus for rows 2 and 4 we have  $S \rightarrow P_1$ ,  $P_1 \rightarrow S$ , and  $P_3 \rightarrow D$  in Eq. (2). The cross section  $I$  can be obtained immediately from  $I = \langle \psi_f^\dagger, \psi_f \rangle$ , and the polarization  $\underline{P}$  from  $\underline{IP} = \langle \psi_f^\dagger, \underline{\sigma} \psi_f \rangle$ . Substituting  $\psi_f = M \chi_i$  and taking spin sums, one obtains  $I'$  (the prime referring to the cross section from a polarized initial state) and  $\underline{IP}$  (for an unpolarized initial state) listed in columns 3 and 4. Here  $I = |A|^2 + |B|^2$ , and  $\underline{P}_i = \langle \chi_i^\dagger, \underline{\sigma} \chi_i \rangle$  is the initial-state polarization (zero for our bubble chamber). It is seen that the four possibilities can be resolved by measuring both the left-right asymmetry in the angular distribution of  $\Sigma$ 's produced from polarized protons and the polarization of  $\Sigma$ 's from unpolarized protons. However, in our case we know the initial state to be a well-defined mixture of  $S$  and  $D$  waves with a small addition of  $P_1$ .<sup>1</sup> This removes the necessity of an experiment with a polarized initial state, reducing the four-fold ambiguity of Table I to a choice between rows 2 and 3. The determination of the  $\Sigma$  parity becomes a matter of measuring the sign of the polarization term.

One further ambiguity arises, resulting from the fact that the operation of complex conjugation of the final-state wave function, like the Minami transformation  $\underline{\sigma} \cdot \underline{k}_f$ , leaves  $I$  invariant but changes the sign of  $\underline{P}$ . We are fortunate however, in dealing with a narrow resonance to which the Wigner theorem is applicable.<sup>4</sup> This theorem, a consequence of causality, states that the phase shift,  $\eta$  of a resonant state cannot decrease rapidly as a function of energy when passing through a resonance, unless the radius of interaction is large. For our resonance, the radius of interaction would have to be of the order of 15 fermis for a negative  $d\eta/dE$  to be acceptable. Since complex conjugation reverses the

sign of  $dn/dE$ , the ambiguity associated with complex conjugation does not exist for a narrow resonance.<sup>5</sup>

As shown later, our data indicate row 2 to be the proper choice, so let us write explicitly for  $I$  and  $\underline{IP}$

$$I = \frac{\pi \lambda^2}{4\pi} [ |P_1 + (S+2D) \cos \theta|^2 + |(S-D)|^2 \sin^2 \theta ] \quad (3)$$

$$\underline{IP} = \frac{\pi \lambda^2}{4\pi} 2 \operatorname{Im}(S-D)^* [P_1 + (S+2D) \cos \theta] \sin \theta \underline{n} \quad (4)$$

The various amplitudes and phases in the  $\Sigma^\pi$  reactions are determined in the following manner. Below resonance, the incoming  $K^-p$  S-state dominates all other waves. Here the  $\Sigma^+$ ,  $\Sigma^-$ , and  $\Sigma^0$  corresponding amplitudes are given by  $S^+ = S_0/\sqrt{3} - S_2/\sqrt{2}$ ,  $S^- = S_0/\sqrt{3} + S_1/\sqrt{2}$ ,  $S^0 = -S_0/\sqrt{3}$ , where  $S_0$  and  $S_1$  are the S-wave amplitudes in the isotopic spin-0 and -1 states. The magnitudes of  $S_0$  and  $S_1$  at the resonance are determined by extrapolating the nonresonant  $\Sigma^0$  cross section for  $S_0$  and the  $\Sigma^+ + \Sigma^- - 2\Sigma^0$  cross section for  $S_1$ . We obtain  $|S_0| = 0.48$  and  $|S_1| = 0.61$  at resonance. These values are in good agreement with the zero-effective-range Humphrey-Ross solution I and also satisfy unitarity with respect to the other channels.<sup>1</sup> The relative phase angle between  $S_0$  and  $S_1$  can be determined from the difference between the  $\Sigma^+$  and  $\Sigma^-$  cross sections. For  $K^-$  capture at rest this phase angle is 60 deg, and at about 250-Mev/c incident  $K^-$  momentum passes through 90 deg, increasing slowly with momentum. By extrapolating to the 395-Mev/c resonance momentum, we estimate the angle to be  $\approx 110$  deg. Beyond the resonance, P-waves become appreciable, so that an interpolation to the resonance would be less reliable. In what follows we shall consider these values of  $S_0$  and  $S_1$  and their phase angle as constants throughout the resonance region. Now, in the vicinity of the resonance we introduce into the  $I_0$  state a D-wave amplitude of the Breit-Wigner form

$$D = \frac{\left[ \frac{2}{3} \frac{\Gamma_{\Sigma}}{\Gamma} \left( 1 - \frac{\Gamma_{\Sigma} + \Gamma_{\Lambda}}{\Gamma} \right) \right]^{1/2}}{\epsilon - i} \quad (5)$$

where  $\Gamma = \Gamma_N + \Gamma_{\Sigma} + \Gamma_{\Lambda}$ ,  $\epsilon = \frac{2}{\Gamma} (E_r - E)$ ,  $E_r$  is the resonance energy and  $\Gamma_N$ ,  $\Gamma_{\Sigma}$ , and  $\Gamma_{\Lambda}$  are the partial decay rates into  $\bar{K}N$ ,  $\Sigma\pi$ , and  $\Lambda_2\pi$ , respectively. The values of  $\Gamma_N$ ,  $\Gamma_{\Sigma}$ , and  $\Gamma_{\Lambda}$  have been previously established from enhancements in the various channels at resonance.<sup>1,6</sup> This leads to an amplitude  $D = 0.36/(\epsilon - i)$ . It is easily seen that  $D$  is a vector in the complex plane, starting from the origin, the end point of which describes a circle. The orientation of the  $S$  amplitude with respect to the circle is the only free parameter left to be adjusted, and this is done by fitting the angular-distribution terms arising from interference between  $S$  and  $D$ . This orientation of  $S_0$  and  $S_1$  is shown in Fig. 1 with the two circles giving the quantities  $2D$  and  $-D$  of Eqs. (3) and (4). The Wigner theorem excludes the complex conjugate of Fig. 1 which would reverse the sign of  $\underline{F}$ . The distance squared from the point marked  $\Sigma^+$  to the end points of the two vectors  $2\underline{D}$  and  $-\underline{D}$  give, by the use of Eq. (3), the coefficients of  $\cos^2\theta$  and  $\sin^2\theta$  in the  $\Sigma^+$  angular distribution. In a similar manner one obtains the coefficients for the  $\Sigma^-$  and  $\Sigma^0$  angular distributions.<sup>7</sup> We have adjusted the orientation of  $S$  to give the best fits to the  $\Sigma^+$ ,  $\Sigma^-$ , and  $\Sigma^0$  angular distributions as a function of momentum, as shown in Fig. 2. Here we have plotted the experimental ratios  $(P-E)/(P+E)$  and  $(F-B)/(F+B)$ , (here  $P$ ,  $E$ ,  $F$ , and  $B$  are the number of events in the polar, equatorial, front, and back region, respectively. For example, for  $P$  we take  $|\cos\theta| > 0.5$ ) together with the values predicted by Fig. 1 through

$$\frac{P-E}{P+E} = \frac{|S+2D|^2 - |S-D|^2}{4[|S|^2 + |P_1|^2 + 2|D|^2]} \quad (6)$$

The over-all agreement, while not perfect, is very encouraging, considering the simplicity of the analysis. Perhaps the addition of a small amount of  $P_3$  (interfering with  $P_1$ ) would improve the fits, the restriction to  $J = 1/2$  in the P state being somewhat artificial. The curves have been extended well beyond the resonance to illustrate the behavior of the interference, although far from resonance the S-wave amplitudes should change appreciably and the Breit-Wigner formula will have a more involved energy dependence.

The  $\sin\theta \cos\theta$  term in Eq. (4) results from interference between S and D waves and therefore is now uniquely specified for all three  $\Sigma$  channels. To determine the average value of the polarization arising from this term, we consider a sample of events for which the c.m. production angle is  $0.3 \leq |\cos\theta| \leq 0.95$ . Over this interval  $\overline{\sin\theta \cos\theta}$  is 0.43. We then obtain  $\overline{(\alpha \bar{P})}$  for the forward and backward c.m. angles from  $\overline{(\alpha \bar{P})} = 3 \sum_i \cos\beta_i$ , where  $\cos\beta_i = \underline{n} \cdot \underline{k}_p$ ,  $\underline{k}_p$  being the direction of the decay proton in the hyperon center of mass and  $\alpha$  the proton helicity. We then have

$$(\alpha \bar{P})_{\sin\theta \cos\theta} = \frac{1}{N} [(\overline{(\alpha \bar{P})})_{\text{forward}} - (\overline{(\alpha \bar{P})})_{\text{backward}}] \quad (7)$$

for the average value of this polarization term over the  $\cos\theta$  interval, where  $N$  is the number of events. For the sign of  $\alpha$ , we use the determination of Beall et al.<sup>8</sup> This experiment shows that the proton in  $\Sigma_0^+$  decay has negative helicity (i.e. the proton is emitted preferentially opposite to the direction of the  $\Sigma$  polarization), whereas the other decay modes of charged  $\Sigma$  are consistent with zero helicity. For the decay  $\Sigma^0 \rightarrow \Lambda + \gamma$ , one has  $\underline{P}_\Lambda = -(1/3) \underline{P}_{\Sigma^0}$  and experiments now indicate that protons from  $\Lambda$  decay have positive helicity.<sup>9</sup> In both cases we take  $|\alpha| = 1$ . From Eq. (7) we then obtain the values of  $(\alpha \bar{P})_{\sin\theta \cos\theta}$  reported in Fig. 3a (for  $\Sigma^0$ ) and 3b (for  $\Sigma_0^+$ ). The calculated curves are those predicted for odd  $KP\Sigma$  parity. For the other parity assumption, the signs of the calculated curves should be reversed, clearly disagreeing with the data.

The result of this experiment, when compared to the  $K^- + \text{He}$  experiment which yields odd  $K\Lambda$  parity,<sup>10</sup> shows that the relative  $\Sigma\Lambda$  parity is even, thereby experimentally establishing the assumption made in many symmetry models of baryons.<sup>11</sup>

The presence of a front-back ratio different from zero in the angular distributions of Fig. 2 implies an interference between odd and even orbital states. This requires that a certain amount of P waves be introduced into the  $\Sigma\pi$  production amplitude in addition to the S and resonant D wave. The presence of P-waves manifests itself also in the coefficient of the  $\sin\theta$  term of  $\underline{IP}$ . We compute the value of this coefficient by considering an interval  $|\cos\theta| \leq 0.95$  over which  $\overline{\sin\theta} = 0.82$ , and using the relation

$$(\overline{aP})_{\sin\theta} = \frac{1}{N} [(\overline{IaP})_{\text{forward}} + (\overline{IaP})_{\text{backward}}] . \quad (8)$$

The values so obtained are shown in Fig. 3a and b for the  $\Sigma^0$  and  $\Sigma_0^+$ , respectively. For the  $\Sigma^+\pi^-$  channel the requisite P-wave cross section is about 1.5 mb. The other  $\Sigma\pi$  channels yield less information concerning the P wave, but we surmise that the cross sections at 395 Mev/c are about 1.5 mb in each of the two isospin states. This gives us the P-wave contribution to the total cross section to be introduced into Eq. (5). The  $\Lambda\pi$  channel appears to contain about an equal amount of S and P waves. Together, the  $\Sigma$  and  $\Lambda$  P-wave absorptions yield the observed small P wave in the  $K^-p$  and  $\bar{K}^0n$ .<sup>1</sup>

It is appropriate now to enumerate some minor flaws in the interpretation developed here and in the previous Letter. These pertain to the  $\Sigma\pi$  absorption cross sections in the three charge channels. The width of the  $\Sigma^0\pi^0$  resonance absorption as a function of momentum seems too large to be accounted for by the experimental resolution; however, since this reaction is observed indirectly,<sup>1</sup> the uncertainty associated with it is greater than with other channels. Secondly, the cross-section enhancements in the three  $\Sigma\pi$  channels seem to be slightly different,  $\Sigma^+\pi^-$  and  $\Sigma^-\pi^+$  being respectively higher and lower than  $\Sigma^0\pi^0$ . Perhaps

the latter effect could arise from mass difference or from the presence of a small  $I_1, D_{3/2}$  absorption. However the over-all internal consistency in the experiment seems so good that such discrepancies can hardly alter the conclusion of odd  $KP\Sigma$  parity.

Analysis is still in progress. A least-squares fit to all the data employing appropriate momentum dependences of the various amplitudes is under way in an effort to improve our primitive fits. Experimental details and final results will be reported in a later paper.

It is a pleasure to acknowledge the support of Professor Luis W. Alvarez. We are indebted to Professors Richard H. Dalitz, Murray Gell-Mann and Henry P. Stapp for valuable discussions, and to Professor Richard H. Capps whose original considerations<sup>12</sup> stimulated our attention to these phenomena. Thanks are also due to the other members of this collaborative experiment-- P. L. Bastien, J. P. Berge, O. I. Dahl, J. Kirz, D. H. Miller, A. H. Rosenfeld and particularly to Dr. J. J. Murray for his excellent beam design.

## FOOTNOTES AND REFERENCES

\* Work done under the auspices of the U. S. Atomic Energy Commission.

† National Academy of Sciences Fellow.

1. M. Ferro-Luzzi, R. D. Tripp, M. B. Watson, Phys. Rev. Letters (to be published).
2. S. Minami, Progr. Theoret. Phys. 11, 213 (1954). Generalization of the Minami transformation has been discussed, for example, in a paper by M. Nauenberg and A. Pais, Phys. Rev. 123, 1058 (1961).
3. We neglect the simultaneous presence of two  $J = 3/2$  states of opposite parity, since no  $\cos^3 \theta$  terms are detected in any angular distribution. The  $D_{3/2}$  state is abbreviated as D.
4. E. P. Wigner, Phys. Rev. 98, 145 (1955).
5. In a recent preprint, R. H. Capps discusses similar problems in connection with the 1520-Mev resonance and in addition considers generalized Yang-type ambiguities. He concludes that ambiguities of this type are improbable, since they would require a rapid variation of more than one partial wave in passing through the resonance. We thank Professor Capps for correspondence and for communicating his results to us prior to publication.
6. Since the resonance is narrow and the c.m. momentum high ( $\sim 260$  Mev/c), in this simplified treatment we neglect any momentum dependence of the decay rates.
7. The  $\Sigma^0$  angular distribution is inferred from the angular distribution of lambdas that lie in a kinematic region inaccessible to  $\Lambda\pi^0$  and  $\Lambda\pi^0\pi^0$  production. The subsequent decay,  $\Sigma^0 \rightarrow \Lambda + \gamma$ , alters the angular distribution, but the effect is slight relative to the statistical uncertainty.

8. E. F. Beall, B. Cork, D. Keefe, P. G. Murphy, W. A. Wenzel, Phys. Rev. Letters 7, 285 (1961).
9. R. W. Birge and W. B. Fowler, Phys. Rev. Letters 5, 254 (1960); and reference 8.
10. M. M. Block, F. Anderson, A. Pevsner, E. Harth, J. Leitner, and H. Cohn, Phys. Rev. Letters 3, 291 (1959).
11. See for example: M. Gell-Mann, Phys. Rev. 106, 1296 (1957); J. S. Schwinger, Ann. Phys. 2, 407 (1957); A. Pais, Phys. Rev. 110, 574 (1958).
12. R. H. Capps, Phys. Rev. Letters 6, 375 (1961).

Table I. Generalized Minami ambiguities.

Transition matrix M	Parity of M	Cross section $I'$	$I \underline{P}$	Example initial $\rightarrow$ final
$(A + B \underline{\sigma} \cdot \underline{n})$	+	$I + I \underline{P} \cdot \underline{P}_i$	$2 \operatorname{Re}(A^* B) \underline{n}$	$SP_1 P_3 \rightarrow SP_1 P_3$
$\underline{\sigma} \cdot \underline{k}_f (A + B \underline{\sigma} \cdot \underline{n}) \underline{\sigma} \cdot \underline{k}_i$	+	$I + I \underline{P} \cdot \underline{P}_i$	$-2 \operatorname{Re}(A^* B) \underline{n}$	$P_1 SD \rightarrow P_1 SD$
$(A + B \underline{\sigma} \cdot \underline{n}) \underline{\sigma} \cdot \underline{k}_i$	-	$I - I \underline{P} \cdot \underline{P}_i$	$2 \operatorname{Re}(A^* B) \underline{n}$	$P_1 SD \rightarrow SP_1 P_3$
$\underline{\sigma} \cdot \underline{k}_f (A + B \underline{\sigma} \cdot \underline{n})$	-	$I - I \underline{P} \cdot \underline{P}_i$	$-2 \operatorname{Re}(A^* B) \underline{n}$	$SP_1 P_3 \rightarrow P_1 SD$

## FIGURE LEGENDS

Fig. 1. Geometrical construction of the S- and D- wave amplitudes of Eqs. (3) and (4). The vectors  $\vec{S}_0$  and  $\vec{S}_1$  are assumed to remain constant throughout the momentum region in the neighborhood of the resonance. The direction and magnitude of the vector  $2\vec{D}$  is obtained as a function of momentum from the upper circle; values of the momentum (in Mev/c) are indicated on the periphery of the circle.

Fig. 2. Momentum dependence of the  $\Sigma^0$ ,  $\Sigma^-$ ,  $\Sigma^+$  angular distributions.

(a), (b), and (c). The "(polar-equatorial)/(polar+equatorial)" ratios for a total of 163 neutral, 860 negative, and 1335 positive  $\Sigma$ 's, respectively.

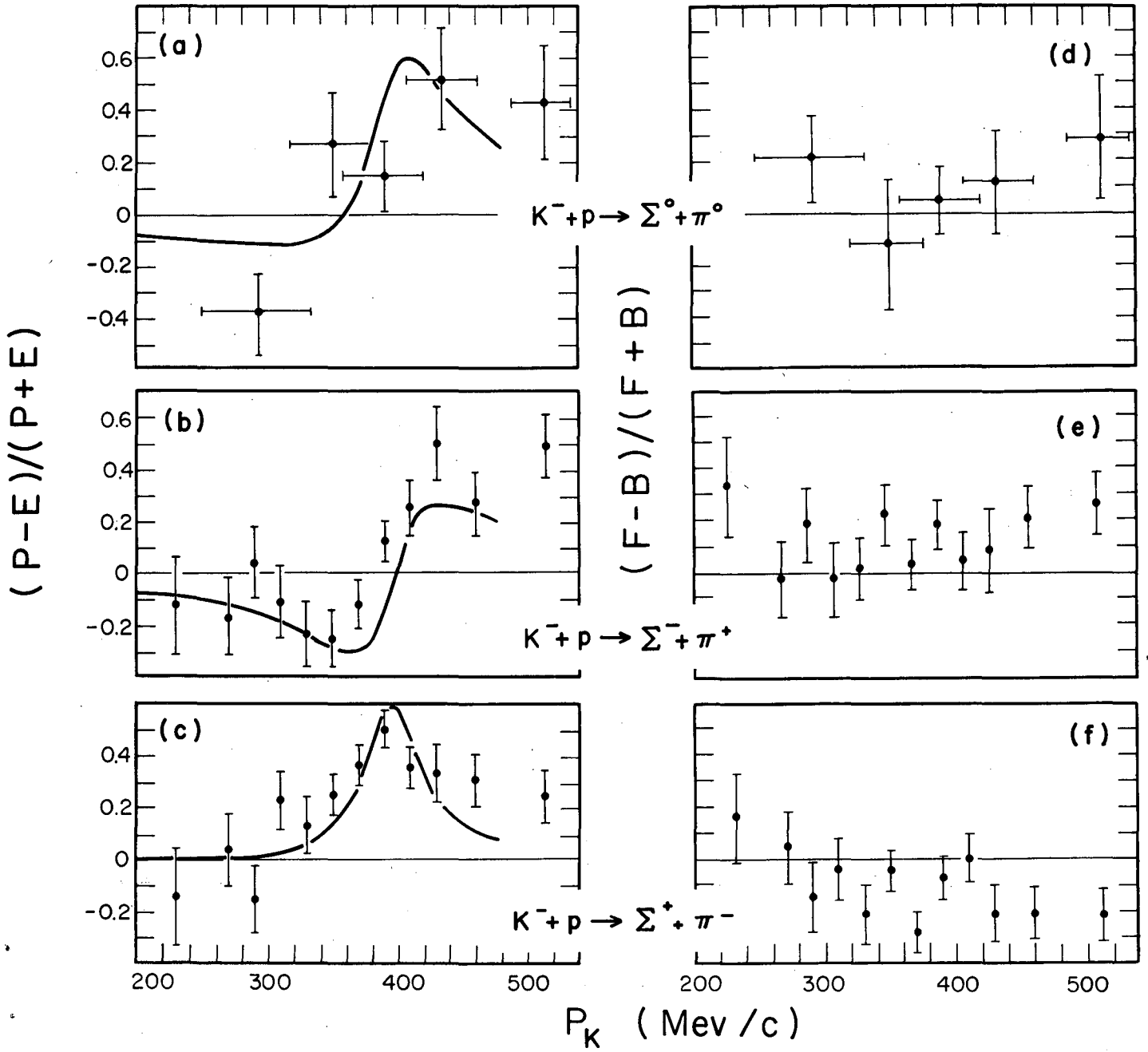
(d), (e) and (f). The "(forward - backward)/(forward+backward)" ratios for the same events. The curves are derived from Eq. (3) and Fig. 1. Errors represent the statistical uncertainty.

Fig. 3. Momentum dependence of the polarization terms.

(a) and (b). The  $\sin\theta \cos\theta$  term of the polarization, as measured by the use of Eq. (7), for a total of 610  $\Sigma^+ \rightarrow p + \pi^0$  decays and 163  $\Sigma^0 \rightarrow \Lambda + \gamma$  followed by  $\Lambda \rightarrow p + \pi^-$  decays. The curves represent the predictions obtained from Eq. (4) and Fig. 1.

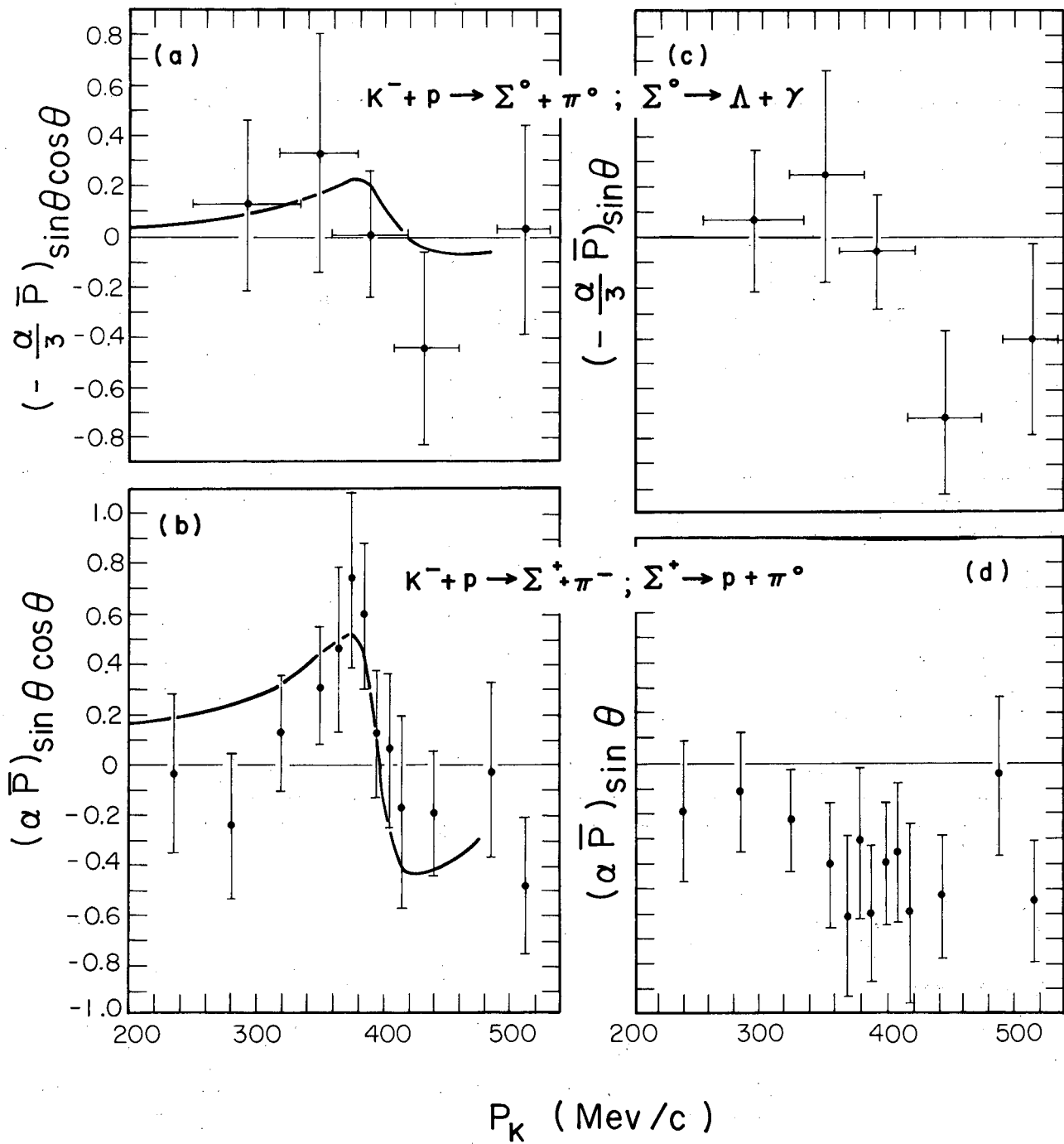
(c) and (d). The  $\sin\theta$  term of the polarization, as measured by the use of Eq. (8), for the same events.





MUB-894

Fig. 2



MUB-895

Fig. 3

This report was prepared as an account of Government sponsored work. Neither the United States, nor the Commission, nor any person acting on behalf of the Commission:

- A. Makes any warranty or representation, expressed or implied, with respect to the accuracy, completeness, or usefulness of the information contained in this report, or that the use of any information, apparatus, method, or process disclosed in this report may not infringe privately owned rights; or
- B. Assumes any liabilities with respect to the use of, or for damages resulting from the use of any information, apparatus, method, or process disclosed in this report.

As used in the above, "person acting on behalf of the Commission" includes any employee or contractor of the Commission, or employee of such contractor, to the extent that such employee or contractor of the Commission, or employee of such contractor prepares, disseminates, or provides access to, any information pursuant to his employment or contract with the Commission, or his employment with such contractor.